Casein Kinase 2 Regulates the NR2 Subunit Composition of Synaptic NMDA Receptors

Antonio Sanz-Clemente[1], **Jose A. Matta**[2], **John T.R. Isaac**[2], and **Katherine W. Roche**[1,*]

[1]Receptor Biology Section, National Institute of Neurological Disorders and Stroke (NINDS), National Institutes of Health, Bethesda, MD 20892

[2]Synaptic Plasticity Section, National Institute of Neurological Disorders and Stroke (NINDS), National Institutes of Health, Bethesda, MD 20892

SUMMARY

NMDA receptors (NMDARs) play a central role in development, synaptic plasticity and neurological disease. NMDAR subunit composition defines their biophysical properties and downstream signaling. Casein kinase 2 (CK2) phosphorylates the NR2B subunit within its PDZ-binding domain; however, the consequences for NMDAR localization and function are unclear. Here we show that CK2 phosphorylation of NR2B regulates synaptic NR2B and NR2A in response to activity. We find that CK2 phosphorylates NR2B, but not NR2A, to drive NR2B-endocytosis and remove NR2B from synapses resulting in an increase in synaptic NR2A expression. During development there is an activity-dependent switch from NR2B to NR2A at cortical synapses. We observe an increase in CK2 expression and NR2B phosphorylation over this same critical period, and show that the acute activity-dependent switch in NR2 subunit composition at developing hippocampal synapses requires CK2 activity. Thus CK2 plays a central role in determining the NR2 subunit content of synaptic NMDARs.

INTRODUCTION

N-methyl-D-aspartate receptors (NMDARs) are a subtype of ionotropic glutamate receptors, which are widely expressed throughout the nervous system. NMDARs play important roles in development, learning and memory, as well as in some neuropsychiatric disorders (Lau and Zukin, 2007). The NMDAR subunits (NR1, NR2A-D and NR3A-B) assemble as tetramers containing two NR1 subunits and two NR2 (or NR3) subunits to form functional NMDARs (Cull-Candy and Leszkiewicz, 2004; Furukawa et al., 2005). In particular, NMDARs in cerebral cortex are primarily composed of two NR1 subunits, and two NR2A or NR2B subunits (Al-Hallaq et al., 2007; Kohr, 2006; Tovar and Westbrook, 1999).

Protein composition and receptor density at synapses are strongly regulated by several mechanisms including phosphorylation and interactions with PDZ domain-containing proteins (Chen and Roche, 2007; Kim and Sheng, 2004; Kim and Huganir, 1999). For example, phosphorylation of the PDZ-binding domain of the inwardly rectifying K^+ channels Kir2.3 and Kir5.1 by cAMP-dependent protein kinase disrupts their association

[*]Correspondence: Katherine W. Roche (rochek@ninds.nih.gov), National Institute of Neurological Disorders and Stroke (NINDS), National Institutes of Health, Bldg. 35, Room 2C903, 9000 Rockville Pike, Bethesda, MD 20892, Tel. 301 496-3800; Fax 301 480-4186.

with PSD-95 and modulates their function (Cohen et al., 1996; Tanemoto et al., 2002). In addition, AMPA receptor internalization is regulated by protein kinase C, which directly phosphorylates the PDZ binding domain of GluR2 (S880) and prevents its association with GRIP, but not with PICK1 (Chung et al., 2003; Perez et al., 2001; Seidenman et al., 2003). The NR2B subunit of NMDARs is also phosphorylated within its PDZ binding domain, on serine 1480 (S1480). Casein kinase 2 (CK2) phosphorylates S1480, disrupts the interaction of NR2B with PSD-95 and SAP102, and leads to a decrease in NR2B surface expression. Interestingly, phosphorylation of NR2B on S1480 is regulated by synaptic activity and CaMKII (Chung et al., 2004), but the impact of CK2 phosphorylation on synaptic NMDARs has not been evaluated.

CK2 is a highly conserved serine/threonine kinase, organized as a tetramer composed of two catalytic subunits (α and α') and two regulatory β subunits (Litchfield, 2003; Pinna and Meggio, 1997). Although it is constitutively active, CK2 activity can be modulated by a diverse array of stimuli, and a number of mechanisms contribute to CK2 regulation *in vivo*, including interaction with proteins and small molecules, phosphorylation and regulated expression and assembly (Blanquet, 2000; Faust and Montenarh, 2000; Litchfield, 2003; Litchfield et al., 1994). Although ubiquitous, the activity of CK2 is 3–8 fold higher in brain than in non-neuronal tissues, and, in particular, cortex and hippocampus express high levels of CK2 (Blanquet, 2000; Girault et al., 1990; Martin et al., 1990). Little is known about the function of this kinase in the nervous system, but studies suggest a role in learning and memory (Blanquet, 2000). For example, LTP transiently increases CK2 activity in hippocampus (Charriaut-Marlangue et al., 1991).

The subunit composition of synaptic NMDARs in forebrain changes during development and this switch is activity-dependent (Barria and Malinow, 2002; Bellone and Nicoll, 2007; Carmignoto and Vicini, 1992; Quinlan et al., 1999). During early development, NR2B-containing NMDARs are predominant, whereas NR2A-containing NMDARs become abundant by adulthood. However, the precise molecular mechanisms mediating the switch remain obscure. We now show that CK2 differentially phosphorylates NR2A and NR2B. In addition, CK2 modulates the synaptic expression of NR2 subunits, increasing the level of synaptic NR2A and decreasing synaptic NR2B via increased endocytosis. Finally, CK2 regulates NR2B phosphorylation during development and is required for the NR2B to NR2A switch induced by activity in young animals, showing that CK2 is a key regulator of NR2 subunit composition of synaptic NMDARs.

RESULTS

NR2B is phosphorylated by CK2 within the PDZ ligand on S1480, which disrupts its association with PDZ domain-containing proteins (Chung et al., 2004). The extreme C-termini of NR2A and NR2B share a high degree of homology and, in particular, their 6 last amino acids (a.a.), including the PDZ binding domain (-ESDV), are identical (Figure 1A). Therefore, we tested if NR2A was phosphorylated by CK2 on S1462, the analogous serine within its PDZ binding domain. We performed *in vitro* phosphorylation assays, using GST fusion proteins containing the last 175 a.a. of NR2A and NR2B, both wild type (wt) and mutants to disrupt the phosphorylation (GST-NR2A S1462A and GST-NR2B S1480A). GST-proteins were incubated with $[\gamma\text{-}^{32}P]$ATP and CK2 +/− 25 µM TBB, a selective CK2 inhibitor (Sarno et al., 2001; Sarno et al., 2005), as described in Experimental Procedures. NR2B was robustly phosphorylated by CK2, and the S1480A mutation completely abolished the phosphorylation. Furthermore, incubation with TBB inhibited ^{32}P incorporation. However, strikingly, NR2A was not efficiently phosphorylated by CK2 *in vitro* (Figure 1B).

To evaluate the phosphorylation of endogenous NR2 subunits by CK2 *in vivo*, we performed a back phosphorylation assay. We first treated cortical neurons +/− 25 µM TBB to inhibit CK2, which should reduce the endogenous phosphorylation of CK2 substrates. After cell lysis, NR2A or NR2B was immunoprecipitated using specific antibodies and subjected to an *in vitro* phosphorylation assay with CK2 as described above. ^{32}P incorporation into NR2B was more robust when isolated from TBB-treated neurons than when isolated from control cultures (Figure 1C), consistent with the reduced CK2 phosphorylation of endogenous NR2B after TBB-treatment. In contrast we observed no specific signal in NR2A immunoprecipitates, either control or TBB-treated, showing that endogenous NR2A is not efficiently phosphorylated by CK2.

An important consequence of NR2B phosphorylation on Ser1480 is the disruption of PDZ interactions. To determine if CK2 activity modulates the association of NR2A and NR2B with PDZ-containing proteins, we performed co-immunoprecipitation experiments in HEK293 cells transfected with PSD-95, NR1, and NR2A or NR2B. After treatment with 25 µM TBB for 4 hours, we observed an increase in the association of PSD-95 with NR2B, as predicted. However, TBB treatment did not increase the binding of PSD-95 to NR2A (Figure 1D). The association of NR2A or NR2B with NR1, evaluated as control, was not affected by TBB (data not shown). Taken together, these data show that, despite its high homology with NR2B, the NR2A C-terminus is a poor substrate for CK2 and, accordingly, CK2 activity regulates NR2B, but not NR2A, binding to PDZ domain-containing proteins.

Our data showing that CK2 differentially regulates NR2A and NR2B prompted us to investigate the role of CK2 in the trafficking and synaptic localization of these subunits. First, we analyzed the effect of inhibiting CK2 activity on the surface expression of the NR2A and NR2B. We treated cortical neurons (DIV 10) with 25 µM TBB and performed cell surface biotinylation assays as described in the Experimental Procedures. Consistent with previous studies (Chung et al., 2004), we observed an increase in the surface expression of NR2B in the cultures treated with TBB (Figure 2A). In contrast, the level of NR2A expressed on the cell surface was dramatically reduced with the same treatment (Figure 2A). CK2 activity did not modify AMPA receptor surface expression. In addition, we used a fluorescence-based assay and confocal microscopy to visualize receptor surface expression. Hippocampal neurons expressing GFP-NR2A or GFP-NR2B were treated with TBB and surface-expressed receptors were labeled with anti-GFP antibody. Consistent with our biochemical results, neurons treated with TBB showed a significant reduction in the ratio of surface NR2A compared to the total amount of NR2A and, in contrast, an increase in NR2B surface expression (Figure 2B).

We next investigated if CK2 activity also regulates the synaptic expression of NR2 subunits. Thus, we analyzed the synaptic localization of GFP-NR2A and GFP-NR2B after TBB-treatment using immunofluorescence microscopy to measure the colocalization with PSD-95, a classical postsynaptic marker. We observed a decrease in the colocalization of NR2A with PSD-95 in TBB-treated hippocampal neurons, as well as an increase in the colocalization of PSD-95 with NR2B (Figure 2C).

Based on these findings, we conclude that CK2 differentially regulates the surface expression and synaptic localization of NR2 subunits in an inverse manner, increasing the level of NR2A-containing and decreasing NR2B-containing NMDARs. Similar results were observed using DRB, an additional CK2 inhibitor (Figure S1), confirming the role of CK2 in NR2 regulation.

CK2 is a pleiotropic kinase, which phosphorylates several proteins present at synapses that could potentially modulate synaptic expression of NMDAR subunits (Blanquet, 2000). To

investigate whether the effects observed after CK2 inhibition are caused by the direct phosphorylation of NR2B within its PDZ binding domain, we generated a non-phosphorylatable mutant of NR2B. Mutation of S1480 to Ala prevents phosphorylation, but also disrupts the interaction of NR2B with PSD-95 family members (Lim et al., 2002; Prybylowski et al., 2005) making results obtained from this mutant difficult to interpret. However, we found that mutating E1479 to Gln (position −4 in the PDZ binding domain) eliminates CK2 phosphorylation, whereas binding to PDZ domain-containing proteins is retained. As shown in Figure 3A, NR2B E1479Q is not phosphorylated by CK2 in an *in vitro* phosphorylation assay. However, pull-down experiments performed incubating the last 175 a.a. of NR2B attached to GST with lysates of HEK293 cells expressing PSD-95 or SAP102 showed that NR2B E1479Q retains the ability to bind to MAGUK proteins. As expected, two mutants with a defective PDZ-domain, either containing a phosphomimetic mutation (NR2B S1480E) or truncation (NR2B V1482Stop), showed no binding to MAGUK proteins, confirming the specificity of our assay (Figure 3B; data for SAP102 not shown).

Therefore, we used the phosphorylation deficient mutant NR2B E1479Q to study whether S1480 phosphorylation of NR2B regulates the surface and synaptic expression of NR2B. We quantified surface-expressed receptors and the colocalization with PSD-95 in hippocampal neurons transfected with GFP-NR2B wt or GFP-NR2B E1479Q as described for Figure 2. Strikingly, we found that the level of the non-phosphorylatable mutant of NR2B present at the cell surface was dramatically elevated (Figure 3C). Furthermore, it exhibited an increased colocalization with PSD-95 (Figure 3D).

In addition, we generated and analyzed the analogous mutant for NR2A, NR2A E1461Q. In contrast to NR2B, NR2A E1479Q was very similar to wild-type NR2A in both the level of surface expression and its colocalization with PSD-95 (Figures 3C and 3D). These results demonstrate that the ratio of synaptic NR2B is regulated via S1480 phosphorylation and that the analogous residue of NR2A does not regulate synaptic NR2A expression.

We next investigated the mechanisms underlying the regulation of NR2B trafficking by CK2. One likely possibility is that the observed decrease in surface and synaptic expression is due to increased NMDAR endocytosis. This hypothesis is supported by the fact that CK2 activity disrupts the binding of NR2B with MAGUK proteins (Figure 1D and (Chung et al., 2004) and it has been demonstrated that PSD-95 stabilizes NMDARs at the surface and inhibits endocytosis (Lavezzari et al., 2003). Therefore, we analyzed the effect of CK2 on NMDAR endocytosis using a fluorescence-based trafficking assay in GFP-NR2B- or GFP-NR2B E1479Q-transfected neurons (Suh et al., 2008). Surface receptors were labeled with anti-GFP antibody and the cells returned to 37 °C for 30 minutes to allow protein internalization (+/− TBB). After incubating with Alexa-568 conjugated secondary antibody (shown in green), cells were permeabilized and the internalized pool of receptors was visualized with Alexa-633 conjugated secondary antibody (white). The endocytosis of NR2B is strongly reduced by the inhibition of CK2 (Figure 4A). Interestingly, we also observed a decrease in the endocytosis of the phosphorylation deficient mutant NR2B E1479Q that was not further decreased by the presence of TBB. These findings show that CK2 reduces NR2B internalization via S1480 phosphorylation (Figure 4A). Consistent with our previous findings, endocytosis of NR2A E1461Q was the same as NR2A wt (Figure S2).

Several motifs have been identified in NMDAR subunits that regulate endocytosis (Lau and Zukin, 2007). Among them, the tyrosine-based endocytic motif (YEKL) present in the extreme C-terminus of NR2B is a prime candidate to be affected by CK2 activity because of its close proximity to S1480 (Figure 1A). In addition, there is an interplay between the binding of MAGUK proteins with NR2B via the PDZ-domain and the phosphorylation of

the YEKL motif (Y1472) that results in the stabilization of NMDARs in the membrane (Lavezzari et al., 2003; Prybylowski et al., 2005). Therefore, we tested whether phosphorylation in the PDZ domain of NR2B regulates its surface expression and endocytosis via phosphorylation of Y1472. We generated NR2B constructs with mutations in both the PDZ-binding domain (E1479Q or S1480E) and in the YEKL endocytic motif (Y1472A). As expected, we observed reduced internalization for the NR2B Y1472A mutant (Lavezzari et al., 2004; Prybylowski et al., 2005). Strikingly the level of endocytosis of NR2B E1479Q was almost indistinguishable from NR2B Y1472A. Most important, the double mutant, NR2B Y1472A;E1479Q, did not show any additional decrease in endocytosis, indicating that the phosphorylation in the PDZ domain and in the YEKL motif share a common molecular mechanism to reduce NR2B endocytosis. Consistently, the increased endocytosis of NR2B S1480E was decreased to the levels of NR2B Y1472A by introducing an additional mutation in the YEKL motif (NR2B Y1472A;S1480E). Similar levels of endocytosis were observed with NR2B E1479Q and NR2B Y1472A;E1479Q (Figure 4B). Accordingly, we found that the mutation in the YEKL motif did not modify the surface expression of NR2B E1479Q, whereas it did significantly increase the surface levels of the phosphomimetic S1480E to the levels obtained by the non-phosphorylatable NR2B E1479Q mutant (Figure 4C).

The findings of these immunofluorescence experiments suggest that phosphorylation in the PDZ binding domain of NR2B affects the phosphorylation of the YEKL endocytic motif, which increases NMDARs internalization. To examine this hypothesis, we investigated the effect of CK2 inhibition on Y1472 phosphorylation. We analyzed the levels of NR2B pY1472 and pS1480 in HEK293 transfected with PSD-95, NR1 and NR2B after incubation +/− 25 µM TBB for 4 hours. As expected, we observed a reduction in NR2B pS1480 and a concomitant increase in Y1472 phosphorylation (Figure 4D).

It is well known that the subunit composition of synaptic NMDARs changes during development. During early postnatal development, NR2B-containing NMDARs predominate, whereas NR2A-containing NMDARs are the major synaptic subtype in the adult central nervous system (Groc et al., 2009; Lau and Zukin, 2007). Thus far our data demonstrate that CK2 can modify the NR2A/2B ratio of synaptic NMDARs, so we hypothesized that CK2 might be important in the developmental switch of NR2 subunit composition. The fact that CK2 activity is developmentally regulated (Blanquet, 2000) and is modulated by synaptic activity (Charriaut-Marlangue et al., 1991) makes it a good candidate. Therefore, we evaluated the expression of CK2, NR2A, NR2B and NR2B S1480 phosphorylation during development by immunoblotting extracts of cortical synaptosomes from mice at different ages. As previously reported (Petralia et al., 2005; van Zundert et al., 2004) we observed a substantial increase in NR2A and a slight decrease in NR2B expression throughout development. Remarkably, we found that S1480 phosphorylation (evaluated as a ratio to total NR2B) is elevated in the second postnatal week, the critical period for replacement of NR2B by NR2A (Figure 5A and 5B). We also analyzed the levels of CK2 catalytic and regulatory subunits (alpha and beta, respectively) and found that both subunits reached their highest level of expression during the critical period for the NR2 subunit switch (P11–15) (Figure 5A and 5C). The accessibility of CK2 to the substrate can play a major role in regulation of CK2 phosphorylation (Faust and Montenarh, 2000). Therefore, we used subcellular fractionation and immunoblotting to see if CK2 is enriched at SPMs along with NR2 subunits. We found that the association of CK2 alpha and beta subunits with the SPM at P13 was dramatically elevated in comparison with younger or older tissue, supporting a role for this kinase in synaptic development (Figure 5D and 5F). Consistent with our previous data, the level of NR2B pS1480 was elevated in P13 in SPM and pY1472 was reduced in comparison with the adult levels (Figure 5D and 5E).

The synaptic incorporation of NR2A requires synaptic activity and can be blocked by NMDAR inhibitors (Barria and Malinow, 2002; Bellone and Nicoll, 2007). As previously reported (Chung et al., 2004), we find that phosphorylation of NR2B on S1480 is induced by activity that is dependent on synaptic NMDAR activation, because we observe a substantial reduction in NR2B S1480 phosphorylation in cultures treated for 8 hours with tetrodotoxin (2 µM) or overnight with NMDAR inhibitors (100 µM APV; 40 µM MK801) (Figures 6A and 6B). Conversely, increasing synaptic activity with bicuculline (40 µM for 8 hours) or KCl (20 mM for 5 min) results in an elevated level of NR2B S1480 phosphorylation compared with control cultures (Figures 6A). In addition, NR2A expression modulates synaptic NR2A by promoting its insertion into synaptic membranes (Barria and Malinow, 2002). Therefore, to investigate whether the level of NR2A expression can also modify NR2BpS1480, we analyzed NR2A knock-out mice by immunoblotting cortical synaptosomes from P11. Interestingly, we found a significant reduction in the amount of NR2B phosphorylated on S1480 in mice lacking NR2A (Figure 6C). Therefore, the same stimuli that are required for the NMDAR switch also regulate NR2B S1480 phosphorylation.

We have substantial evidence that CK2 activity affects synaptic expression of NR2 subunits and that NR2B S1480 is a critical residue. However, is it possible that NR2B is phosphorylated on S1480 by another kinase. To investigate this possibility, we performed an *in vitro* phosphorylation assay with the C-terminus NR2B attached to GST, using 10 µg of brain lysate as source of endogenous kinases. We found that NR2B was phosphorylated *in vitro* upon incubation with the brain lysate, but the phosphorylation was blocked in the presence of 25 µM TBB (Figure 6D) consistent with the phosphorylation of NR2B S1480 being mediated exclusively by CK2.

LTP induction rapidly induces a switch in NMDA receptor subunit composition from NR2B- to NR2A-containing NMDARs at synapses on hippocampal CA1 pyramidal neurons in young (2–9 day-old) rats (Bellone and Nicoll, 2007). We next studied a role for CK2 in this activity-driven switch using whole-cell patch-clamp recordings from CA1 pyramidal neurons in acute hippocampal slices prepared from 4–9 day-old rats. Consistent with previous work (Bellone and Nicoll, 2007), an LTP induction protocol caused the speeding of NMDA receptor EPSC decay and a decrease in ifenprodil (5 µM) block that was specific to the pathway in which the LTP protocol was applied (Figure 7A–C, G, H). These findings confirm that activity causes a rapid switch from NR2B-containing NMDA receptors, which exhibit slow decay kinetics and are blocked by ifenprodil, to NR2A-containing NMDA receptors that exhibit faster kinetics and a lack of ifenprodil sensitivity. To determine if CK2 is involved in this subunit composition switch, in experiments interleaved with the controls (described above) we incubated slices in TBB (10 µM) for at least two hours and then tested the ability of activity to drive the subunit switch. In TBB-treated slices, the LTP induction protocol failed to cause a speeding of NMDA EPSC kinetics or reduce sensitivity to ifenprodil (Figure 7D–F, G, H). Thus CK2 is involved in the activity-dependent switch in NR2 subunit composition of synaptic NMDA receptors.

DISCUSSION

Many functional properties of NMDARs are determined by NR2 subunits, including affinity for glutamate, sensitivity to Mg^{2+}, single channel conductance, open probability and deactivation time (Furukawa et al., 2005; Groc et al., 2009). Not surprisingly, NR2 subunits are subject to strict control mechanisms and the NR2A and NR2B subunits are differentially regulated. For instance, these subunits show distinct patterns of expression during the development and, in adult brain, NR2B is restricted to forebrain whereas NR2A is ubiquitously expressed (Kohr, 2006; Monyer et al., 1994; Wenzel et al., 1997). NR2A and

NR2B also exhibit a different subcellular localization. In cortex and hippocampal pyramidal cells NR2A is highly localized to postsynaptic membranes whereas there is a high amount of NR2B at extrasynaptic sites (Kew et al., 1998; Scimemi et al., 2004; Tovar and Westbrook, 1999). Trafficking of NR2A and NR2B is also differentially modulated, as NR2B-containing receptors are more dynamic than NR2A, with a higher rate of endocytosis (Lavezzari et al., 2004), lateral diffusion (Groc and Choquet, 2006) and, a higher association with recycling endosomes (Lavezzari et al., 2004) compared to NR2A.

Phosphorylation is one of the major regulatory mechanisms for NMDARs. Both subunits are substrates for a number of kinases, although differences between subunits also exist (Chen and Roche, 2007). In this study, we show differential regulation of synaptic NR2A and NR2B by CK2. It has been reported that CK2 phosphorylates NR2B within the PDZ binding domain (Chung et al., 2004). We now show that CK2 phosphorylates NR2B much more efficiently than NR2A, which leads to a decrease in synaptic expression of NR2B. In addition, we have characterized a NR2B mutant that cannot be phosphorylated by CK2, but maintains the binding with MAGUK proteins (NR2B E1479Q). We found that this mutant mimics the effect of CK2 inhibition in altering both NR2B surface expression and colocalization with PSD-95, indicating that the phosphorylation in the PDZ binding domain of NR2B by CK2 regulates receptor trafficking. Futhermore, we have identified an interplay between S1480 phosphorylation and the YEKL endocytic motif, providing a molecular mechanism for the observed effects on NMDAR trafficking. Our findings support a model in which the coordinated phosphorylation of two different residues of NR2B: S1480 within the PDZ domain binding domain and Y1472 within the tyrosine-based YEKL endocytic motif regulates receptor endocytosis, and ultimately the surface expression of NR2B (Figure 8). Specifically, the association of NR2B with MAGUK proteins, such as PSD-95, is disrupted when NR2B is phosphorylated by CK2 within its PDZ binding domain (S1480). The disruption of this interaction triggers a decrease in Y1472 phosphorylation of NR2B within the YEKL endocytic domain and, ultimately, an increase in NR2B internalization by association with AP-2 (Blanpied et al., 2002; Chung et al., 2004; Prybylowski et al., 2005; Roche et al., 2001). This model is based on our analyses of NR2B constructs with mutations in the YEKL and/or PDZ binding domain and on the quantification of Y1472 and S1480 phosphorylation on NR2B after pharmacological inhibition of CK2. In addition, this model is entirely consistent with previous studies showing that increased PSD-95 binding to NR2B leads to increased Y1472 phosphorylation and NR2B surface expression (Song et al., 2003; Zhang et al., 2008). In addition, it has been recently reported that chronic ethanol treatment in cultured neurons results in a decrease in NR2B S1480 phosphorylation and leads to a NR2B translocation from synaptic to extrasynaptic sites (Clapp et al., 2010). Although a very similar treatment with ethanol also decreases NR2B Y1472 phosphorylation (Alvestad et al., 2003) this is likely due to a pathologically elevated tyrosine-phosphatase activity (Xu et al., 2003; Zhao and Zhang, 1996) rather than a coordinated mechanism between the YEKL and PDZ binding domain.

We also show that NR2B Y1472A, which is unable to bind to the clathrin adaptor protein AP-2, exhibits reduced endocytosis, and accordingly, increased surface expression. These results are consistent with previous studies in which different stimuli that reduce Y1472 phosphorylation also decrease NR2B surface expression (Snyder et al., 2005; Zhang et al., 2008). However, Prybylowski et al reported that NR2B Y1472A shows increased synaptic but not total surface expression, based on their current density recording in response to applied NMDA (Prybylowski et al., 2005). This discrepancy with our current findings could be due to the use of cerebellar granular cells (CGCs) for the electrophysiological studies in the manuscript by Prybylowski et al., because the authors found a significant increase of NR2B Y1472A surface expression when analyzed in hippocampal cultures by immunocytochemistry in the same study.

We find that NR2A, like NR2B, is strongly regulated by CK2 activity. However, NR2B is an excellent substrate for CK2, whereas NR2A is not (Figure 1). We mutated E1479Q on NR2B to block CK2 phosphorylation and found this eliminated the effect of CK2 inhibition on NR2B internalization. However, the analogous mutation on NR2A (NR2A E1461Q) showed the same ratio of endocytosis as wild type NR2A. These data all suggest that CK2 activity affects NR2A trafficking via an indirect modulation by phosphorylating other synaptic proteins. This mechanism would include an increase in NR2A stabilization in postsynaptic membranes, the delivery to synapses or even modulation of NR2A expression (Groc et al., 2009;Perez-Otano and Ehlers, 2005). MAGUK proteins such as PSD-95 (Soto et al., 2004), kinases such as PKC (Allende and Allende, 1995) or PKA (Carmichael et al., 1982;Hemmings et al., 1982), phosphatases such as PP2A (Heriche et al., 1997), PP2C (Pinna and Meggio, 1997) or PTP1B (Jung et al., 1998) and a large number of transcription factors (Blanquet, 2000;Meggio and Pinna, 2003) are some of the candidate proteins phosphorylated by CK2 that might affect NR2A synaptic expression. An alternative and appealing explanation for our observations is that the NMDAR 2A/2B subunit switch is a mechanism with two sequential and coupled stages, in which the synaptic removal of NR2B is required to allow NR2A synaptic incorporation. CK2, therefore, might facilitate NR2A insertion by removing NR2B from the synaptic sites via S1480 phosphorylation (Figure 8). All our data are consistent with such a model.

Our findings reveal an important role for CK2 in regulating synaptic NMDARs. CK2 is a ubiquitous serine/threonine kinase that is highly expressed in the brain, where it is widely distributed in both neuronal and non-neuronal cells (Allende and Allende, 1995; Blanquet, 2000; Pinna, 1990). CK2 activity is high in cortex and, interestingly, 25–30% of its total activity is localized in the synaptosomal fraction (Girault et al., 1990). It is not clear what function CK2 is performing at synapses, but increasing evidence suggests a role in learning and memory. For example, LTP can be blocked by CK2 inhibitors (5,6-dichloro-1-β-D-ribofuranosyl-benzimidazole - DRB - and TBB) by reducing NMDAR activity (Kimura and Matsuki, 2008). Furthermore, DRB is able to reduce fear-motivated learning (Igaz et al., 2002). In addition to NR2B, a large number of proteins associated with synaptic plasticity has been reported to be phosphorylated by CK2 (Blanquet, 2000). Consistently, extracts of the frontal cortex of Alzheimer's disease patients show a decreased level of this kinase (Aksenova et al., 1991). However, a recent study reported an increase on spatial learning after inhibition of CK2 using dominant-negative mutants (Chao et al., 2007). Notably, CK2 is developmentally regulated. Its activity is high at embryonic day 16 in cortex, remains elevated during the early postnatal period and decreases slightly in the adult. However, in liver, CK2 activity decreases around birth (Girault et al., 1990). Those data and our findings that the highest expression levels of CK2 and its association with synaptic plasma membranes are reached at P11–15 suggest a developmental role for CK2.

The NMDAR subunit switch is one of the more studied events during synaptic maturation. It is well established that synaptic NR2B-containing NMDARs are replaced by NR2A-containing during the second postnatal week in rodents, a process that has been studied extensively in visual cortex (Carmignoto and Vicini, 1992; Hestrin, 1992; Philpot et al., 2001; Quinlan et al., 1999; van Zundert et al., 2004). It is known that NR2A incorporation into postsynaptic membranes is dependent on synaptic activity and the level of NR2A expression (Barria and Malinow, 2002), but the molecular mechanisms controlling the NMDAR switch remain unclear. Remarkably, it has been reported recently that induction of LTP in young animals (2–9 days old) results in a rapid replacement of synaptic NR2B subunits by NR2A, as demonstrated by faster kinetics and a lower inhibition by ifenprodil obtained in the LTP path compared to the control (Bellone and Nicoll, 2007). However, no molecular mechanism has been implicated in mediating these effects. We now find CK2 activity is an important step for this switch. We have demonstrated that CK2 differentially

regulates synaptic NMDAR subunits, increasing NR2A and reducing NR2B, and, in addition, CK2 activity is known to increase rapidly during the induction of LTP in hippocampus (Charriaut-Marlangue et al., 1991). Importantly, we have shown that the NMDAR subunit switch induced by LTP is blocked in the presence of a CK2 inhibitor. Consistent with this hypothesis, both the switch and NR2B S1480 phosphorylation by CK2 are dependent on synaptic activity and NMDAR activation. How activity modulates NR2B S1480 phosphorylation is unclear, but it is known that it is partially dependent on CaMKII (Chung et al., 2004 and data not shown). Although CaMKII can phosphorylate the CK2 beta subunit directly, this phosphorylation does not modify NR2B S1480 phosphorylation in an *in vitro* phosphorylation assay (Chung et al. 2004). One possibility is that CaMKII phosphorylation of CK2 targets CK2 to the synaptic plasma membrane, allowing the interaction with NR2B (see the coincident increased of NR2B S1480 phosphorylation and association of CK2 with SPMs at P13 in Figure 5D–F). Identifying the molecular mechanisms underlying the spatiotemporal regulation of synaptic CK2 activity is an important topic for future investigation as our data demonstrate that CK2 strongly regulates synaptic NMDARs composition.

EXPERIMENTAL PROCEDURES

Neuronal cultures, antibodies and reagents

Primary cultured neurons were prepared from E18 Sprague-Dawley rats as previously described (Roche and Huganir, 1995). For biochemical experiments we used cortical neurons because the cortex yields enough material for biochemical analyses, whereas hippocampal cultures are the preferred for immunocytochemistry. The use and care of animals used in this study followed the guidelines of the NIH Animal Research Advisory Committee. C-terminal NR2B, synaptophysin, and CK2 subunit beta antibodies were purchased from Sigma (St. Louis, MO). We obtained phosphorylation state-specific S1480 NR2B antibody from Pierce (Rockford, IL), NR2A from Upstate (Lake Placid, NY), actin from Applied Biological Materials (Richmond, BC, Canada) and EEA1 from BD Biosciences (San Jose, CA). GluR1 and phosphorylation state-specific Y1472 NR2B antibody were from Chemicon (Billerica, MA). NR1, PSD-95 and CK2 subunit alpha antibodies were purchased from Affinity BioReagents (Golden, CO). Anti-GFP and all secondary antibodies for immunofluorescence were obtained from Invitrogen (-Molecular Probes- Eugene, OR). All the drugs and inhibitors used in this study were purchased from Tocris Cookson (Ellisville, MO) except APV and picrotoxin (Sigma - St. Louis, MO) and DRB (Calbiochem -San Diego, CA). GFP-NR2A and GFP-NR2B constructs were kindly provided by Dr. Stefano Vicini (Georgetown University).

Isolation of the neuronal membrane fraction and biotinylation assay of surface-expressed receptors

For the preparation of the crude membrane fraction, cortical neurons were harvested in cold PBS/Ca^{2+} (PBS, 0.1 mM $CaCl_2$) and collected by centrifugation. The pellet was resuspended in hypotonic buffer (20 mM Tris pH 8.8 ; 5 mM EDTA ; 1 mM Na_3VO_4) with protease and phosphatase inhibitors (Roche and Sigma, respectively), briefly sonicated and centrifuged again at 20,000× g for 20 min at 4°C. After SDS-PAGE, the samples were immunoblotted with the indicated antibodies. The same membrane was re-blotted for the analysis of NR2B phospho / total ratio. For the biotinylation assay, cultures were washed three times in cold PBS+ (PBS ; 1 mM $MgCl_2$; 0.1 mM $CaCl_2$) and incubated with 1 mg/ml EZ-Link Sulfo-NHS-SS-Biotin (Pierce) in PBS+ for 15 min at 4°C. After quenching the reaction with 100 mM glycine in PBS+ at 4°C for 10 min, the total membrane fraction was isolated as described above. Membranes were solubilized in 1% SDS for 15 min at 37 °C, diluted with 10 volumes of cold PBS/1% TX-100 and centrifuged for 45 min at 100,000× g.

The supernatant was then incubated with Streptavidin beads (Thermo Scientific) for 2 hours at 4 °C and, after four washes, bound proteins were immunoblotted with the indicated antibodies. Data are presented as mean +/− SEM and significance was analyzed using the student's t test. Experiments were repeated at least three times, independently.

Subcellular fractionation of brain tissue

Biochemical fractionation was performed following standard methods (Hallett et al., 2008). Briefly, cortex from mice of different developmental stages was homogenized in cold TEVP buffer (10 mM Tris pH 7.5 ; 1 mM EDTA ; 1 mM EGTA ; 1 mM Na_3VO_4) containing 0.32 M sucrose and phosphatase and protease inhibitors. Homogenate was centrifuged 10 min to 1,000× g at 4 °C to remove nuclei and large debris. The supernatant (SN1) was centrifuged to 10,000× g to obtain the crude synaptosome (P2) fraction. P2 was incubated in hypoosmotic solution (20 mM Tris pH 8.8 ; 5 mM EDTA ; 1 mM Na_3VO_4) for 20 min on ice and centrifuged 30 min at 25,000× g to obtain synaptic plasma membranes (SPMs). Tissue was collected and processed three times independently and the protein expression analyzed twice for each tissue collection.

Co-immunoprecipitation and pull-down assays

HEK293T cells were co-transfected with PSD-95, NR1 and GFP-NR2A or GFP-NR2B (ratio 1:5:10) using the calcium phosphate method following manufacturer's instructions (Clontech). After 24 hours of expression, cells were lysed in PBS containing 1% TX-100 and briefly sonicated. Lysates were incubated with anti-NR2A or anti-NR2B antibodies and protein A-sepharose beads overnight at 4°C, washed and immunoblotted. For pulldown experiments, HEK293T cells were transfected with PSD-95 or SAP102 and processed as before. Lysates were incubated with GST-NR2B C-terminal (wild-type or mutant) for 2 hours at 4°C. After three washes, bound proteins were immunoblotted for PSD-95 or SAP102 to confirm the protein interaction.

In vitro phosphorylation and back phosphorylation analysis

The last 175 a.a. of NR2A or NR2B were fused to GST and purified as previously described (Chen et al., 2006). Mutants were generated by PCR using the QuikChange site-directed mutagenesis kit (Stratagene) following the manufacturer's instructions. *In vitro* phosphorylation was performed by incubating GST-proteins with 50 units of CK2 (New England BioLabs) and 2 pmol [γ-^{32}P]ATP (3,000 Ci/mmol) for 20 min at 30°C in 50 µl of 20 mM Tris pH 7.5 ; 50 mM KCl ; 10 mM $MgCl_2$; 0.1 mM ATP. For brain lysate phosphorylation, SN1 fraction from adult mice cortex was dissolved in 2% TX-100 with protease inhibitors for 5 min at RT. GST-proteins were incubated with 10 µg of the dissolved SN1 in 20 mM HEPES, pH 7.0, 1.67 mM $CaCl_2$, 1 mM dithiothreitol, 10 mM $MgCl_2$, 0.1 mM ATP and phosphatase inhibitors (Sigma) for 20 min at 30°C. When indicated, 25 µM TBB was added to the reaction. For back phosphorylation, cortical cultures (DIV10) were incubated with 25 µM TBB overnight to reduce endogenous phosphorylation of CK2 substrates. Cells were harvested and lysed with 1 % DOC. After the addition of equal volume of RIPA buffer, receptors were recovered using specific NR2A or NR2B antibodies. The isolated receptors were incubated with 50 units of CK2 as above.

Immunofluorescence

Receptor endocytosis was analyzed using a fluorescence-based antibody uptake assay, as previously reported (Lavezzari et al., 2004; Suh et al., 2008). Briefly, hippocampal neurons were transfected with GFP-NR2A or GFP-NR2B at DIV7 and maintained with 25 µM TBB. At DIV10, surface receptors were labeled with anti-GFP antibody for 15 minutes at room temperature, and returned at 37°C for 30 minutes to allow protein internalization. Surface

proteins were labeled with Alexa 568-conjugated secondary antibody (shown in green). After permeabilization, the internalized pool of receptor was labeled with Alexa 633-conjugated secondary antibody (shown in white). To compare surface-expressed protein versus the intracellular pool, hippocampal neurons were transfected with GFP-NR2A or GFP-NR2B and treated with TBB as above. Surface-expressed receptors were labeled with anti-GFP antibody and Alexa 568-conjugated secondary antibody (shown in white). Cells were permeabilized with 0.25 % TX-100 in PBS and internal pool was labeled with anti-GFP antibody and Alexa 633-conjugated secondary antibody (shown in green). Quantification was performed analyzing the fluorescence intensity of three independent areas per neuron using MetaMorph 6.0 software (Universal Imaging Corp), and is presented as mean +/− SEM. For surface-expression analysis the ratio in the intensity Surface / Intracellular is shown. Data from endocytosis are presented as ratio Internalized / Surface intensities. Colocalization of NR2 subunits and PSD-95 was analyzed in hippocampal neurons (DIV14) transfected as above and maintained with 25 µM TBB. Colocalization level was analyzed using ImageJ and presented as mean +/− SEM. Cells were imaged on a Zeiss LSM 510 confocal microscope. Serial optical sections collected at 0.35 µm intervals were used to create maximum projection images. Experiments were repeated at least, three times independently and significance analyzed using student's t test. n= number of cells.

Electrophysiology

4–9 day-old Wistar rats were anesthetized with isoflurane and decapitated in accordance with NIH animal care and use guidelines. Transverse hippocampal slices (400 µm thick) were cut in ice-cold artificial cerebrospinal fluid (ACSF) containing (mM): 119 NaCl, 2.5 KCl, 2.5 CaCl$_2$, 9 MgSO$_4$, 1 NaH$_2$PO$_4$, 26.2 NaHCO$_3$, 11 glucose equilibrated with 95% O$_2$ and 5% CO$_2$. Slices were allowed to recover for at least one hour in ACSF at room temperature (composition as above except for 1.3 mM MgSO$_4$). Whole cell patch clamp recordings were made from visually identified CA1 pyramidal neurons in the presence of 50 µM picrotoxin at room temperature. The whole-cell solution contained (mM) 115 CsMeSO$_4$, 20 CsCl$_2$, 10 HEPES, 2.5 MgCl$_2$, 4 NaATP, 0.4 NaGTP, 10 NaCreatine, and 0.6 EGTA (pH 7.2).

EPSCs were evoked by electrical stimulation of two independent sets of Schaffer collateral/commissural axons using two bipolar stimulating electrodes placed in stratum radiatum of CA1 (0.1 Hz stimulation frequency for each pathway). The stimulating electrodes were placed on opposite sides of the recorded cell. NMDA receptor EPSCs were obtained in the presence of NBQX (5µM) and picrotoxin (50µM) while cells were voltage-clamped at +40 mV. Recordings were performed using a Multiclamp 700B patch-clamp amplifier (Axon Instruments, Foster City, CA); signals were filtered at 4 kHz, digitized at 10 Hz and displayed and analyzed on-line using pClamp 9.2 (Axon Instruments). For induction of the activity-dependent switch in the subunit composition of synaptic NMDA receptors, an LTP induction protocol was employed, similar as previously described (Bellone and Nicoll, 2007). Cells were voltage clamped at 0 mV while Schaffer collateral/commissural axons were stimulated at 1Hz for 120 seconds. Cells were then voltage-clamped at −70 mV for 5 minutes following LTP induction. Following these 5 minutes, NMDA receptor EPSCs were once again recorded at +40 mV. The EPSC decay is fit with a double exponential function using OriginLab software (Northampton, MA) and decay kinetics are expressed as a weighted decay time constant. Statistical significance was tested using a student's t-test.

Supplementary Material

Refer to Web version on PubMed Central for supplementary material.

Acknowledgments

REFERENCES

Aksenova MV, Burbaeva GS, Kandror KV, Kapkov DV, Stepanov AS. The decreased level of casein kinase 2 in brain cortex of schizophrenic and Alzheimer's disease patients. FEBS letters. 1991; 279:55–57. [PubMed: 1995343]

Al-Hallaq RA, Conrads TP, Veenstra TD, Wenthold RJ. NMDA di-heteromeric receptor populations and associated proteins in rat hippocampus. J Neurosci. 2007; 27:8334–8343. [PubMed: 17670980]

Allende JE, Allende CC. Protein kinases. 4. Protein kinase CK2: an enzyme with multiple substrates and a puzzling regulation. Faseb J. 1995; 9:313–323. [PubMed: 7896000]

Alvestad RM, Grosshans DR, Coultrap SJ, Nakazawa T, Yamamoto T, Browning MD. Tyrosine dephosphorylation and ethanol inhibition of N-Methyl-D-aspartate receptor function. The Journal of biological chemistry. 2003; 278:11020–11025. [PubMed: 12536146]

Barria A, Malinow R. Subunit-specific NMDA receptor trafficking to synapses. Neuron. 2002; 35:345–353. [PubMed: 12160751]

Bellone C, Nicoll RA. Rapid Bidirectional Switching of Synaptic NMDA Receptors. Neuron. 2007; 55:779–785. [PubMed: 17785184]

Blanpied TA, Scott DB, Ehlers MD. Dynamics and regulation of clathrin coats at specialized endocytic zones of dendrites and spines. Neuron. 2002; 36:435–449. [PubMed: 12408846]

Blanquet PR. Casein kinase 2 as a potentially important enzyme in the nervous system. Progress in neurobiology. 2000; 60:211–246. [PubMed: 10658642]

Carmichael DF, Geahlen RL, Allen SM, Krebs EG. Type II regulatory subunit of cAMP-dependent protein kinase. Phosphorylation by casein kinase II at a site that is also phosphorylated in vivo. The Journal of biological chemistry. 1982; 257:10440–10445. [PubMed: 6286653]

Carmignoto G, Vicini S. Activity-dependent decrease in NMDA receptor responses during development of the visual cortex. Science (New York, N.Y. 1992; 258:1007–1011.

Chao CC, Ma YL, Lee EH. Protein kinase CK2 impairs spatial memory formation through differential cross talk with PI-3 kinase signaling: activation of Akt and inactivation of SGK1. J Neurosci. 2007; 27:6243–6248. [PubMed: 17553997]

Charriaut-Marlangue C, Otani S, Creuzet C, Ben-Ari Y, Loeb J. Rapid activation of hippocampal casein kinase II during long-term potentiation. Proceedings of the National Academy of Sciences of the United States of America. 1991; 88:10232–10236. [PubMed: 1946443]

Chen BS, Braud S, Badger JD 2nd, Isaac JT, Roche KW. Regulation of NR1/NR2C N-methyl-D-aspartate (NMDA) receptors by phosphorylation. The Journal of biological chemistry. 2006; 281:16583–16590. [PubMed: 16606616]

Chen BS, Roche KW. Regulation of NMDA receptors by phosphorylation. Neuropharmacology. 2007; 53:362–368. [PubMed: 17644144]

Chung HJ, Huang YH, Lau LF, Huganir RL. Regulation of the NMDA receptor complex and trafficking by activity-dependent phosphorylation of the NR2B subunit PDZ ligand. J Neurosci. 2004; 24:10248–10259. [PubMed: 15537897]

Chung HJ, Steinberg JP, Huganir RL, Linden DJ. Requirement of AMPA receptor GluR2 phosphorylation for cerebellar long-term depression. Science (New York, N.Y. 2003; 300:1751–1755.

Clapp P, Gibson ES, Dell'acqua ML, Hoffman PL. Phosphorylation regulates removal of synaptic N-methyl-D-aspartate receptors after withdrawal from chronic ethanol exposure. The Journal of pharmacology and experimental therapeutics. 2010; 332:720–729. [PubMed: 20008487]

Cohen NA, Brenman JE, Snyder SH, Bredt DS. Binding of the inward rectifier K+ channel Kir 2.3 to PSD-95 is regulated by protein kinase A phosphorylation. Neuron. 1996; 17:759–767. [PubMed: 8893032]

Cull-Candy SG, Leszkiewicz DN. Role of distinct NMDA receptor subtypes at central synapses. Sci STKE. 2004; 2004:re16. [PubMed: 15494561]

Faust M, Montenarh M. Subcellular localization of protein kinase CK2. A key to its function? Cell and tissue research. 2000; 301:329–340. [PubMed: 10994779]

Furukawa H, Singh SK, Mancusso R, Gouaux E. Subunit arrangement and function in NMDA receptors. Nature. 2005; 438:185–192. [PubMed: 16281028]

Girault JA, Hemmings HC Jr, Zorn SH, Gustafson EL, Greengard P. Characterization in mammalian brain of a DARPP-32 serine kinase identical to casein kinase II. Journal of neurochemistry. 1990; 55:1772–1783. [PubMed: 2145398]

Groc L, Bard L, Choquet D. Surface trafficking of N-methyl-D-aspartate receptors: physiological and pathological perspectives. Neuroscience. 2009; 158:4–18. [PubMed: 18583064]

Groc L, Choquet D. AMPA and NMDA glutamate receptor trafficking: multiple roads for reaching and leaving the synapse. Cell and tissue research. 2006; 326:423–438. [PubMed: 16847641]

Hallett PJ, Collins TL, Standaert DG, Dunah AW. Biochemical fractionation of brain tissue for studies of receptor distribution and trafficking. 2008 Current protocols in neuroscience / editorial board, Jacqueline N. Crawley … [et al *Chapter 1*, Unit 1 16.

Hemmings BA, Aitken A, Cohen P, Rymond M, Hofmann F. Phosphorylation of the type-II regulatory subunit of cyclic-AMP-dependent protein kinase by glycogen synthase kinase 3 and glycogen synthase kinase 5. European journal of biochemistry / FEBS. 1982; 127:473–481. [PubMed: 6293815]

Heriche JK, Lebrin F, Rabilloud T, Leroy D, Chambaz EM, Goldberg Y. Regulation of protein phosphatase 2A by direct interaction with casein kinase 2alpha. Science (New York, N.Y. 1997; 276:952–955.

Hestrin S. Developmental regulation of NMDA receptor-mediated synaptic currents at a central synapse. Nature. 1992; 357:686–689. [PubMed: 1377360]

Igaz LM, Vianna MR, Medina JH, Izquierdo I. Two time periods of hippocampal mRNA synthesis are required for memory consolidation of fear-motivated learning. J Neurosci. 2002; 22:6781–6789. [PubMed: 12151558]

Jung EJ, Kang YS, Kim CW. Multiple phosphorylation of chicken protein tyrosine phosphatase 1 and human protein tyrosine phosphatase 1B by casein kinase II and p60c-src in vitro. Biochemical and biophysical research communications. 1998; 246:238–242. [PubMed: 9600099]

Kew JN, Richards JG, Mutel V, Kemp JA. Developmental changes in NMDA receptor glycine affinity and ifenprodil sensitivity reveal three distinct populations of NMDA receptors in individual rat cortical neurons. J Neurosci. 1998; 18:1935–1943. [PubMed: 9482779]

Kim E, Sheng M. PDZ domain proteins of synapses. Nature reviews. 2004; 5:771–781.

Kim JH, Huganir RL. Organization and regulation of proteins at synapses. Current opinion in cell biology. 1999; 11:248–254. [PubMed: 10209161]

Kimura R, Matsuki N. Protein kinase CK2 modulates synaptic plasticity by modification of synaptic NMDA receptors in the hippocampus. The Journal of physiology. 2008; 586:3195–3206. [PubMed: 18483072]

Kohr G. NMDA receptor function: subunit composition versus spatial distribution. Cell and tissue research. 2006; 326:439–446. [PubMed: 16862427]

Lau CG, Zukin RS. NMDA receptor trafficking in synaptic plasticity and neuropsychiatric disorders. Nature reviews. 2007; 8:413–426.

Lavezzari G, McCallum J, Dewey CM, Roche KW. Subunit-specific regulation of NMDA receptor endocytosis. J Neurosci. 2004; 24:6383–6391. [PubMed: 15254094]

Lavezzari G, McCallum J, Lee R, Roche KW. Differential binding of the AP-2 adaptor complex and PSD-95 to the C-terminus of the NMDA receptor subunit NR2B regulates surface expression. Neuropharmacology. 2003; 45:729–737. [PubMed: 14529712]

Lim IA, Hall DD, Hell JW. Selectivity and promiscuity of the first and second PDZ domains of PSD-95 and synapse-associated protein 102. The Journal of biological chemistry. 2002; 277:21697–21711. [PubMed: 11937501]

Litchfield DW. Protein kinase CK2: structure, regulation and role in cellular decisions of life and death. The Biochemical journal. 2003; 369:1–15. [PubMed: 12396231]

Litchfield DW, Dobrowolska G, Krebs EG. Regulation of casein kinase II by growth factors: a reevaluation. Cellular & molecular biology research. 1994; 40:373–381. [PubMed: 7735311]

Martin ME, Alcazar A, Salinas M. Subcellular and regional distribution of casein kinase II and initiation factor 2 activities during rat brain development. Int J Dev Neurosci. 1990; 8:47–54. [PubMed: 2296847]

Meggio F, Pinna LA. One-thousand-and-one substrates of protein kinase CK2? Faseb J. 2003; 17:349–368. [PubMed: 12631575]

Monyer H, Burnashev N, Laurie DJ, Sakmann B, Seeburg PH. Developmental and regional expression in the rat brain and functional properties of four NMDA receptors. Neuron. 1994; 12:529–540. [PubMed: 7512349]

Perez JL, Khatri L, Chang C, Srivastava S, Osten P, Ziff EB. PICK1 targets activated protein kinase Calpha to AMPA receptor clusters in spines of hippocampal neurons and reduces surface levels of the AMPA-type glutamate receptor subunit 2. J Neurosci. 2001; 21:5417–5428. [PubMed: 11466413]

Perez-Otano I, Ehlers MD. Homeostatic plasticity and NMDA receptor trafficking. Trends in neurosciences. 2005; 28:229–238. [PubMed: 15866197]

Petralia RS, Sans N, Wang YX, Wenthold RJ. Ontogeny of postsynaptic density proteins at glutamatergic synapses. Molecular and cellular neurosciences. 2005; 29:436–452. [PubMed: 15894489]

Philpot BD, Sekhar AK, Shouval HZ, Bear MF. Visual experience and deprivation bidirectionally modify the composition and function of NMDA receptors in visual cortex. Neuron. 2001; 29:157–169. [PubMed: 11182088]

Pinna LA. Casein kinase 2: an 'eminence grise' in cellular regulation? Biochimica et biophysica acta. 1990; 1054:267–284. [PubMed: 2207178]

Pinna LA, Meggio F. Protein kinase CK2 ("casein kinase-2") and its implication in cell division and proliferation. Progress in cell cycle research. 1997; 3:77–97. [PubMed: 9552408]

Prybylowski K, Chang K, Sans N, Kan L, Vicini S, Wenthold RJ. The synaptic localization of NR2B-containing NMDA receptors is controlled by interactions with PDZ proteins and AP-2. Neuron. 2005; 47:845–857. [PubMed: 16157279]

Quinlan EM, Olstein DH, Bear MF. Bidirectional, experience-dependent regulation of N-methyl-D-aspartate receptor subunit composition in the rat visual cortex during postnatal development. Proceedings of the National Academy of Sciences of the United States of America. 1999; 96:12876–12880. [PubMed: 10536016]

Roche KW, Huganir RL. Synaptic expression of the high-affinity kainate receptor subunit KA2 in hippocampal cultures. Neuroscience. 1995; 69:383–393. [PubMed: 8552236]

Roche KW, Standley S, McCallum J, Dune Ly C, Ehlers MD, Wenthold RJ. Molecular determinants of NMDA receptor internalization. Nature neuroscience. 2001; 4:794–802.

Sarno S, Reddy H, Meggio F, Ruzzene M, Davies SP, Donella-Deana A, Shugar D, Pinna LA. Selectivity of 4,5,6,7-tetrabromobenzotriazole, an ATP site-directed inhibitor of protein kinase CK2 ('casein kinase-2'). FEBS letters. 2001; 496:44–48. [PubMed: 11343704]

Sarno S, Ruzzene M, Frascella P, Pagano MA, Meggio F, Zambon A, Mazzorana M, Di Maira G, Lucchini V, Pinna LA. Development and exploitation of CK2 inhibitors. Molecular and cellular biochemistry. 2005; 274:69–76. [PubMed: 16335530]

Scimemi A, Fine A, Kullmann DM, Rusakov DA. NR2B-containing receptors mediate cross talk among hippocampal synapses. J Neurosci. 2004; 24:4767–4777. [PubMed: 15152037]

Seidenman KJ, Steinberg JP, Huganir R, Malinow R. Glutamate receptor subunit 2 Serine 880 phosphorylation modulates synaptic transmission and mediates plasticity in CA1 pyramidal cells. J Neurosci. 2003; 23:9220–9228. [PubMed: 14534256]

Snyder EM, Nong Y, Almeida CG, Paul S, Moran T, Choi EY, Nairn AC, Salter MW, Lombroso PJ, Gouras GK, Greengard P. Regulation of NMDA receptor trafficking by amyloid-beta. Nature neuroscience. 2005; 8:1051–1058.

Song C, Zhang Y, Parsons CG, Liu YF. Expression of polyglutamine-expanded huntingtin induces tyrosine phosphorylation of N-methyl-D-aspartate receptors. The Journal of biological chemistry. 2003; 278:33364–33369. [PubMed: 12810713]

Soto D, Pancetti F, Marengo JJ, Sandoval M, Sandoval R, Orrego F, Wyneken U. Protein kinase CK2 in postsynaptic densities: phosphorylation of PSD-95/SAP90 and NMDA receptor regulation. Biochemical and biophysical research communications. 2004; 322:542–550. [PubMed: 15325264]

Suh YH, Pelkey KA, Lavezzari G, Roche PA, Huganir RL, McBain CJ, Roche KW. Corequirement of PICK1 binding and PKC phosphorylation for stable surface expression of the metabotropic glutamate receptor mGluR7. Neuron. 2008; 58:736–748. [PubMed: 18549785]

Tanemoto M, Fujita A, Higashi K, Kurachi Y. PSD-95 mediates formation of a functional homomeric Kir5.1 channel in the brain. Neuron. 2002; 34:387–397. [PubMed: 11988170]

Tovar KR, Westbrook GL. The incorporation of NMDA receptors with a distinct subunit composition at nascent hippocampal synapses in vitro. J Neurosci. 1999; 19:4180–4188. [PubMed: 10234045]

van Zundert B, Yoshii A, Constantine-Paton M. Receptor compartmentalization and trafficking at glutamate synapses: a developmental proposal. Trends in neurosciences. 2004; 27:428–437. [PubMed: 15219743]

Wenzel A, Fritschy JM, Mohler H, Benke D. NMDA receptor heterogeneity during postnatal development of the rat brain: differential expression of the NR2A, NR2B, and NR2C subunit proteins. Journal of neurochemistry. 1997; 68:469–478. [PubMed: 9003031]

Xu J, Yeon JE, Chang H, Tison G, Chen GJ, Wands J, de la Monte S. Ethanol impairs insulin-stimulated neuronal survival in the developing brain: role of PTEN phosphatase. The Journal of biological chemistry. 2003; 278:26929–26937. [PubMed: 12700235]

Zhang S, Edelmann L, Liu J, Crandall JE, Morabito MA. Cdk5 regulates the phosphorylation of tyrosine 1472 NR2B and the surface expression of NMDA receptors. J Neurosci. 2008; 28:415–424. [PubMed: 18184784]

Zhao Y, Zhang ZY. Reactivity of alcohols toward the phosphoenzyme intermediate in the protein-tyrosine phosphatase-catalyzed reaction: probing the transition state of the dephosphorylation step. Biochemistry. 1996; 35:11797–11804. [PubMed: 8794761]
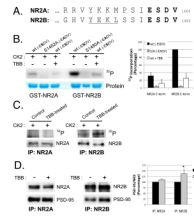
Figure 1. CK2 phosphorylates NR2B much more efficiently than NR2A

A) Alignment of the extreme C-termini of rodent NR2A and NR2B. The PDZ binding domain (-ESDV) is shown in bold and the tyrosine-based endocytic motif in NR2B is underlined in grey. **B**) *In vitro* phosphorylation of the last 175 a.a. of NR2A (1289–1464) or NR2B (1307–1482) by CK2. GST-NR2A, GST-NR2A S1462A, GST-NR2B or GST-NR2B S1480A was incubated with CK2 and [γ-^{32}P]ATP for 20 minutes at 30°C. When indicated, TBB (25 µM) was added to the sample. **C**) Cortical cultures (DIV10) were incubated with 25 µM TBB overnight to reduce endogenous phosphorylation of CK2 substrates. Cells were lysed and receptors recovered using specific NR2A or NR2B antibodies. Immunoprecipitates were subjected to an *in vitro* phosphorylation assay (as in main Figure 1B) with recombinant CK2 for 20 min at 30°C. n=3 **D**) HEK293 cells were co-transfected with PSD-95, NR1, and GFP-NR2A or GFP-NR2B. After treatment with TBB for 4 hours, cells were lysed in PBS with 1% TX-100. The amount of PSD-95 bound to NMDAR subunits was analyzed by co-immunoprecipitation with anti-NR2A or anti-NR2B antibodies. Graph represents means +/− SEM (n=4) *p<0.05
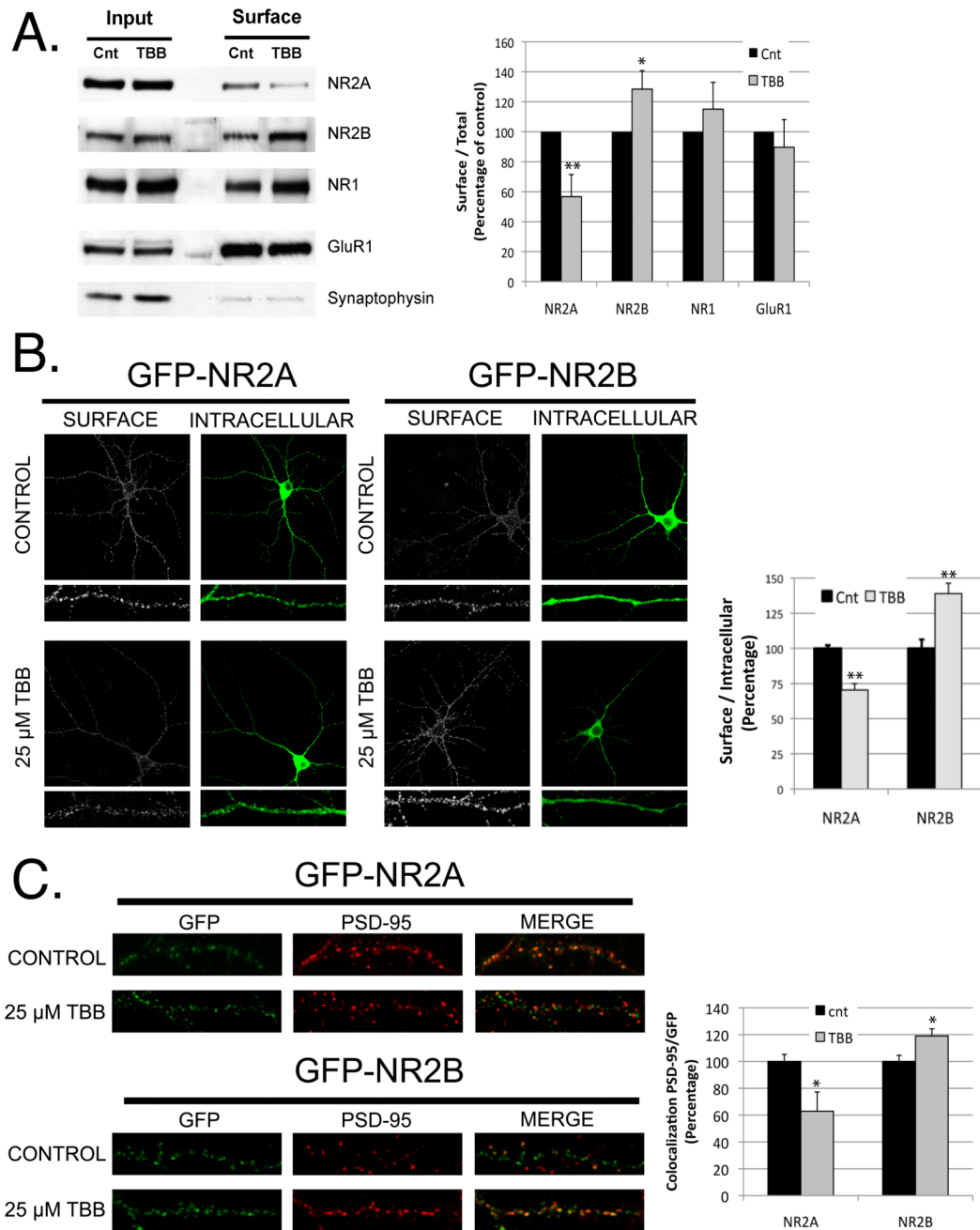
Figure 2. Inhibition of CK2 decreases surface and synaptic NR2A expression, but increases surface and synaptic NR2B

A) Cortical cultures (DIV 10) were treated overnight with 20 µM TBB or vehicle. Surface proteins were biotinylated and isolated with streptavidin-agarose beads as described in Experimental Procedures. Proteins were resolved by SDS-PAGE and blotted for NR2A, NR2B, NR1, GluR1 or synaptophysin (as control). Graph represents means $+/-$ SEM *p < 0.05 **p < 0.01 (n=5) **B**) Hippocampal neurons expressing GFP-NR2A or GFP-NR2B were treated $+/-$ TBB (25 µM). Surface receptors were labeled with anti-GFP antibody and Alexa-568 conjugated anti-rabbit secondary antibody (shown in white). After permeabilization, the internal pool of receptors was visualized by labeling with anti-GFP

and Alexa-633 conjugated anti-rabbit secondary antibody (shown in green). n for NR2A (−/ + TBB) = 21, 16 ; n for NR2B (−/+ TBB) = 17, 22. Data represent means +/− SEM **p < 0.01. **C**) Colocalization of endogenous PSD-95 and NR2B or NR2A was evaluated in hippocampal neurons treated with 25 µM TBB, after transient transfection with GFP-NR2A or GFP-NR2B. n for NR2A(−/+ TBB) = 15, 18 ; n for NR2B (−/+ TBB) = 21, 28. Data represent means +/− SEM *p< 0.05. See also Figure S1
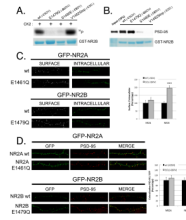
Figure 3. NR2B E1479Q, which is not phosphorylated by CK2, shows increased surface expression and synaptic localization compared to NR2B wt

A) *In vitro* CK2 phosphorylation (as described in Figure 1B) of the last 175 a.a. of NR2B attached to GST (wt, E1479Q, S1480E and V1482Stop) **B**) Pull-down experiments of GST-NR2B (wt, E1479Q, S1480E and V1482Stop). Beads were incubated with lysate of HEK293 cells expressing PSD-95 for 2 hours at 4°C. After washes, the recovered material was analyzed by immunoblotting with an anti-PSD-95 antibody. **C**) Surface expression analysis (as described in Figure 2B) was performed with hippocampal neurons expressing GFP-NR2A (wt or E1461Q) or GFP-NR2B (wt or E1479Q). Graph represents mean +/− SEM ***p<0.001. n for NR2A (wt, E/Q) =25, 21. n for NR2B (wt, E/Q) = 20, 26 **D**) Colocalization of endogenous PSD-95 with GFP-NR2A (wt or E1461Q) and GFP-NR2B (wt or E1479Q) analyzed at DIV14 as indicated in Figure 2C. Graph indicates mean +/− SEM. **p<0.01. n for NR2A (wt, E/Q) =17, 17. n for NR2B (wt, E/Q) = 16, 14.
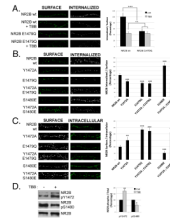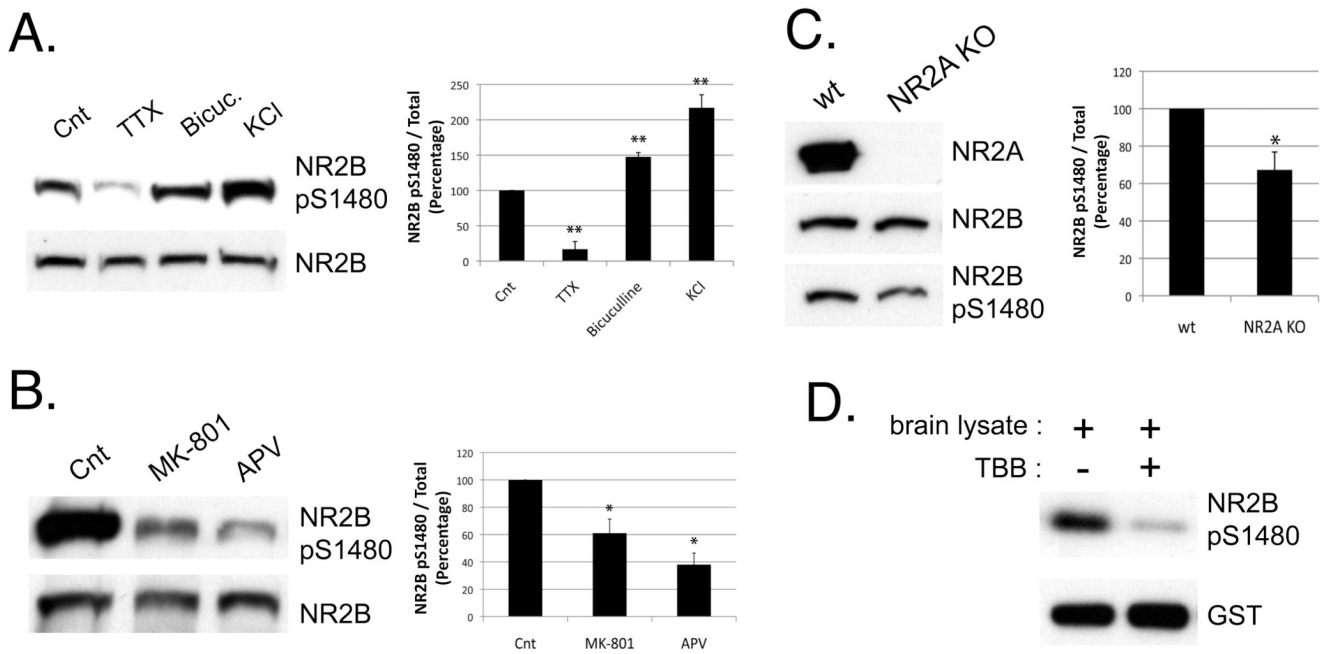
Figure 4. Phosphorylation of NR2B S1480 increases endocytosis via a coordinated dephosphorylation of Y1472 in the YEKL endocytic domain
A) An endocytosis assay of hippocampal neurons transfected with GFP-NR2B (wt or E1479Q) was performed as described in Experimental Procedures. At DIV10, neurons were labeled with anti-GFP antibody, washed and returned to conditioned media (+/− 25 μM TBB) for 30 min at 37 °C to allow receptor internalization. Cells were fixed, and surface-expressed proteins were labeled with Alexa 568-conjugated secondary antibody (shown in green). After permeabilization with 0.25% TX-100, internalized receptors were labeled with Alexa 633-conjugated secondary antibody (shown as white). n for NR2B wt (+/− TBB) = 15, 25. n for NR2B E1479Q (+/− TBB) = 25, 21. Graph represents means +/− SEM ***p<0.001; n.s. denotes not significant differences. **B**) Endocytosis assay with NR2B constructs with mutations in the YEKL and/or PDZ-domain performed as in panel A. n= 31, 25, 29, 27, 15, 26. Graph represents means +/− SEM **p<0.01 ***p<0.001 **C**) Surface expression of NR2B constructs with mutations in the YEKL and/or PDZ-domain was analyzed as in Figure 2B. n= 38, 32, 22, 32, 17, 30. Graph represents means +/− SEM **p<0.01 ; ***p<0.001 **D**) Levels of NR2B phosphorylation (Y1472 and S1480) were analyzed in HEK293T cells transfected with PSD-95, NR1 and GFP-NR2B and incubated +/− 25 μM TBB for 4 hours. n=3. Graph represents means +/−SEM *p<0.05 ; ** p<0.01. See also Figure S2.
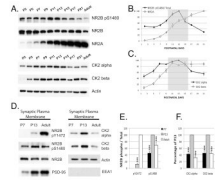
Figure 5. Phosphorylation of NR2B S1480 and total expression of CK2 increase during the second postnatal week. In addition, association of CK2 with synaptic plasma membranes is elevated at P13

A) Protein expression was analyzed in cortical synaptosomes from mice of different stages of development by immunoblotting. Graphs shown in panels **B and C** summarize the data of 6 experiments analyzing the level of NR2B Ser1480 phosphorylation and expression of NR2A and CK2 (alpha and beta subunits) throughout development (the grey area indicates the critical period of time for the NMDAR subunit switch). **D**) Synaptic plasma membranes (SPMs) were isolated from P7, P13 or adult animals, using a standard purification protocol (Hallet, 2008). The level of phosphorylated NR2B (Y1472 and S1480), CK2 (alpha and beta), EEA1 (as negative control) and actin (as loading control) present in the SPMs was analyzed by immunoblotting. **E–F**) Graph represents means +/− SEM ***p<0.001 n=6

Figure 6. Phosphorylation of NR2B on S1480 increases in response to NMDAR-activity and is regulated by NR2A expression

A) Cortical cultures (DIV10) were incubated for 8 hours with Tetrodoxin (TTX; 2 µM) or Bicuculline (Bicuc.; 40 µM) to block or stimulate neuronal activity respectively. Treatment with KCl (20 mM for 5 min) was used to induce neuronal depolarization. The level of phosphorylated NR2B was analyzed by immunoblotting after isolation of cellular membranes. The same membrane was re-blotted for NR2B or phospho-specific NR2B S1480 antibodies. Graph represents means +/− SEM **p<0.01 n=5 **B**) Cortical cultures were incubated overnight +/− NMDAR antagonists (100 µM APV ; 40 µM MK-801). Graph represents means +/− SEM *p<0.05 n=3 **C**) Cortical synaptosomes were isolated from P11 mice (wt or NR2A knock out) and analyzed by immunoblotting with the indicated antibodies. Graph represents means +/− SEM *p<0.05 n=4 **D**) GST-NR2B (last 175 a.a.) was phosphorylated *in vitro* using 10 µg of brain lysate as source of kinases. 25 µM TBB was added to the sample when indicated.
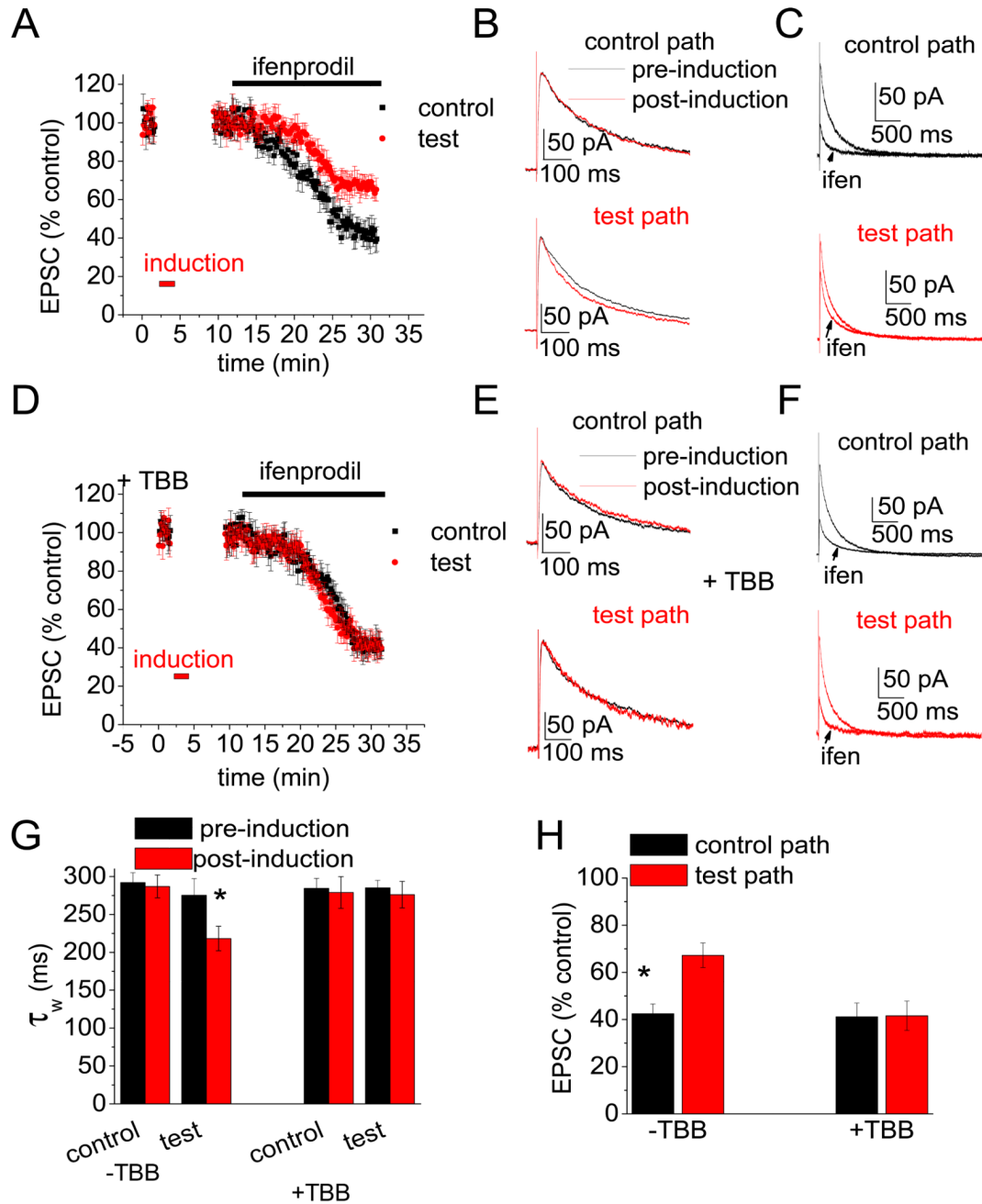
Figure 7. CK2 activity regulates the activity-dependent switch in the subunit composition of synaptic NMDA receptors

A) Pooled data (n = 10) for NMDA EPSC amplitude vs. time from control experiments showing the effect of LTP induction on ifenprodil block (red is test pathway to which the LTP induction protocol was applied; black is the control pathway; these colors are consistent throughout the figure). **B**) NMDA EPSCs from example control experiment showing the speeding of kinetics in test path after induction (lower panel). **C**) NMDA EPSCs from example control experiment showing the reduced block by ifenprodil (5 µM) in test path after induction (lower panel). **D-F**) As for control experiments (A–C), but in slices incubated with TBB (10 µM) for at least 2 hours (n = 7). **G**) Summary data of weighted decay time

constant (control [−TBB] n = 10; +TBB n = 8; * indicates p < 0.05 between pre- and post-induction). **H**) Summary data of NMDA EPSC amplitude in ifenprodil (% of EPSC amplitude in absence of ifenprodil; control [−TBB] n = 10; +TBB n = 7; * indicates p < 0.05 between control and test pathways)
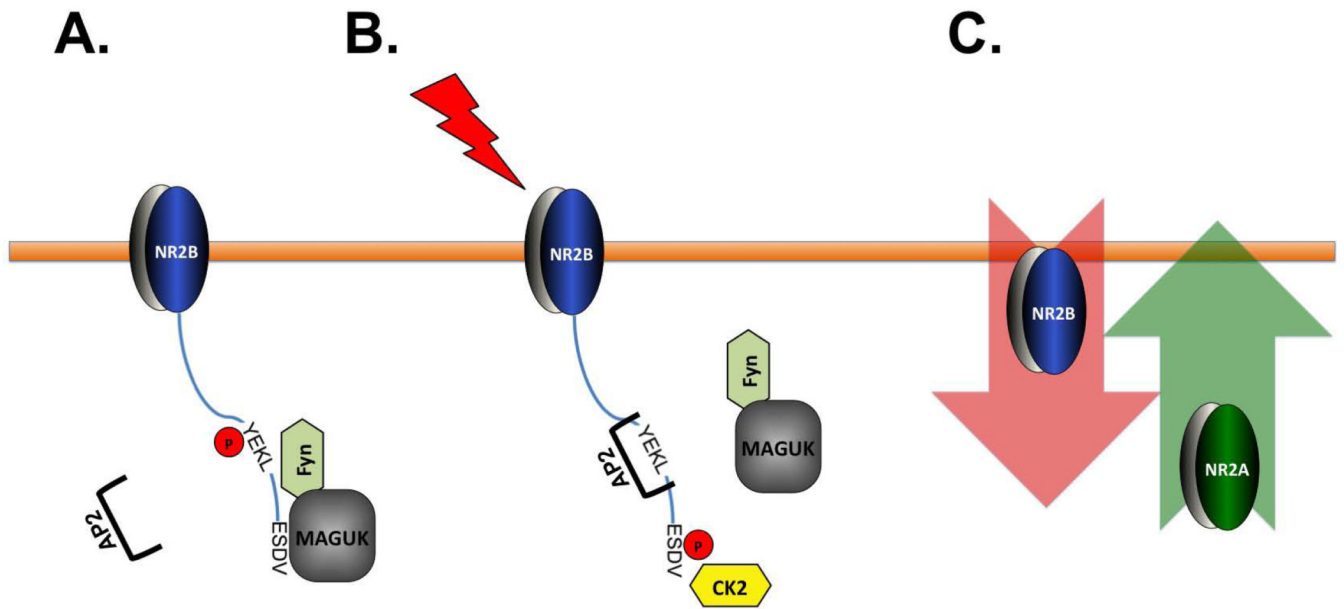
Figure 8. Model of CK2 regulation of synaptic NMDARs
A) Early in development, the association of NR2B with MAGUKs stabilizes NR2B at synaptic membranes via phosphorylation of Y1472 by Fyn. Phosphorylation of the Y1472 within the tyrosine-based endocytic motif blocks AP-2 binding. **B**) During the critical period, NMDAR activity induces NR2B S1480 phosphorylation by CK2, which results in the disruption of NR2B association with MAGUKs. NR2B Y1472 is now dephosphorylated and AP-2 can bind to the YEKL motif and promote NR2B endocytosis. **C**) NR2A expression increases and NR2A-containing receptors replace NR2B-containing NMDARs at synaptic sites.